

Gravity darkening in stars with surface differential rotation

J. Zorec^{1,2}, Y. Frémat^{3,1,2}, A. Domiciano de Souza⁴, F. Royer⁵

¹Sorbonne Universités, UPMC Université Paris 06, Institut d'Astrophysique de Paris, F-75014 Paris, France

²CNRS UMR 7095, Institut d'Astrophysique de Paris, 98bis Bd. Arago, F-75014 Paris, France

³Royal Observatory of Belgium, 3 Av. Circulaire, B-1180 Bruxelles, Belgium

⁴Laboratoire Lagrange, Université Côte d'Azur, Observatoire de la Côte d'Azur, Bd. de l'Observatoire, CS 34229, 06304 Nice Cedex 4, France

⁵GEPI, Observatoire de Paris, PSL Research University, CNRS UMR 8111, Université Paris Diderot, Sorbonne Paris Cité, 5 place Jules Janssen, 92190 Meudon, France



2. Formulation

Since the emerging radiation flux-vector \vec{F} emitted by an axially symmetric stellar atmosphere is anti-parallel to the vector of the local effective gravity \vec{g}_{eff} in radiative envelopes, to a high degree of approximation (Espinosa Lara & Rieutord, 2011, AA, 533, A43) it can be written

$$\vec{F} = -\mathcal{F}(r, \theta)\vec{g}_{\text{eff}}, \quad (1)$$

where (r, θ) are spherical coordinates (r is the radius vector and θ the colatitude angle). The function $\mathcal{F}(r, \theta)$ can then be determined by solving the differential equation describing the condition of radiative equilibrium in the atmosphere (Mihalas 1978, *in* Stellar atmospheres 2nd edition)

$$\nabla \cdot \vec{F} = \vec{g}_{\text{eff}} \cdot \nabla \mathcal{F} + \mathcal{F} \nabla \cdot \vec{g}_{\text{eff}} = 0. \quad (2)$$

With the notation

$$\mathcal{F}(r, \theta) = f(r, \theta) \frac{L}{4\pi GM} \quad (3)$$

and by adopting Maunders' law for the stellar surface angular velocity $\Omega(\theta)$

$$\Omega(\theta) = \Omega_e [1 + \alpha \cos^2(\theta)] \quad (4)$$

where α is the "differential rotation parameter", the solution of Eq. 2 for the function $f(r, \theta)$ becomes

$$f(r, \theta) = \left(\frac{\tan \vartheta}{\tan \theta} \right)^2 \left[\frac{1 + \alpha \cos^2(\vartheta)}{1 + \alpha \cos^2(\theta)} \right]. \quad (5)$$

where $r = r(\theta)$ describes now the geometry of the rotationally deformed stellar surface. The variable $\vartheta = \vartheta(r, \theta, \alpha, \eta)$ is calculated using the characteristics of Eq. 2 which imply that

$$\mathcal{F}(\vartheta) = \frac{1}{3} \eta r^3 \cos^3 \theta + \mathcal{T}(\theta) \quad (6)$$

having $\eta = (\Omega_e/\Omega_c)^2 (R_e/R_c)^3$ and \mathcal{T} a function of θ (right of Eq. 6) and ϑ (left of Eq. 6), whose generic form $\mathcal{T}(x)$ is given by

$$\mathcal{T}(x) = \frac{1}{(1+\alpha)^2} \left[\ln \tan \frac{x}{2} + (1-\alpha) \frac{\arctan(\sqrt{\alpha} \cos x)}{2\sqrt{\alpha}} + \frac{(1+\alpha)}{2} \left(\frac{\cos x}{1+\alpha \cos^2 x} \right) \right], \quad \text{for } \alpha \geq 0 \quad (7)$$

$$= \frac{1}{(1-|\alpha|)^2} \left[\ln \tan \frac{x}{2} + \left(\frac{1+|\alpha|}{4\sqrt{|\alpha|}} \right) \ln \left(\frac{1+\sqrt{|\alpha|} \cos x}{1-\sqrt{|\alpha|} \cos x} \right) + \left(\frac{1-|\alpha|}{2} \right) \left(\frac{\cos x}{1-|\alpha| \cos^2 x} \right) \right], \quad \text{for } \alpha < 0$$

In these equations, it is fundamental to determine the geometrical shape of the star $r = r(\theta)$, which can be calculated as established in Zorec et al (2011, AA, 526, A87).

The gravity darkening can finally be written as

$$T_{\text{eff}}(\theta) = \langle T \rangle [f(\theta)\gamma(\theta)]^{1/4} \quad (8)$$

with $\langle T \rangle^4 = L/4\pi R_c^2 \sigma_{\text{SB}}$ and $\gamma(\theta) = g_{\text{eff}}(\theta)/\langle g \rangle$ is the normalized surface effective gravity. In Fig. 2 is shown $T_{\text{eff}}(\theta)/\langle T \rangle$ as a function of θ for $\eta = 0.8$ and several values of α .

When using the classical expression for the gravity darkening law,

$$\sigma_{\text{SB}} T_{\text{eff}}^4(\theta) = C_{\text{F}} \beta_1(\theta) \langle g \rangle, \quad (9)$$

one of the important consequences introduced by the differential rotation is that the gravity darkening exponent becomes a function of θ AND of α as shown in Fig. 3. Consequently, its value inferred from observations is a function of the stellar inclination angle, i , and is not a genuine parameter reflecting the characteristics of the stellar surface rotation.

1. Motivation

The aim of this poster is to give the expression of the gravity darkening which can be used to calculate the emitted spectrum by a star with surface differential rotation obeying Maunders' relation for the angular velocity.

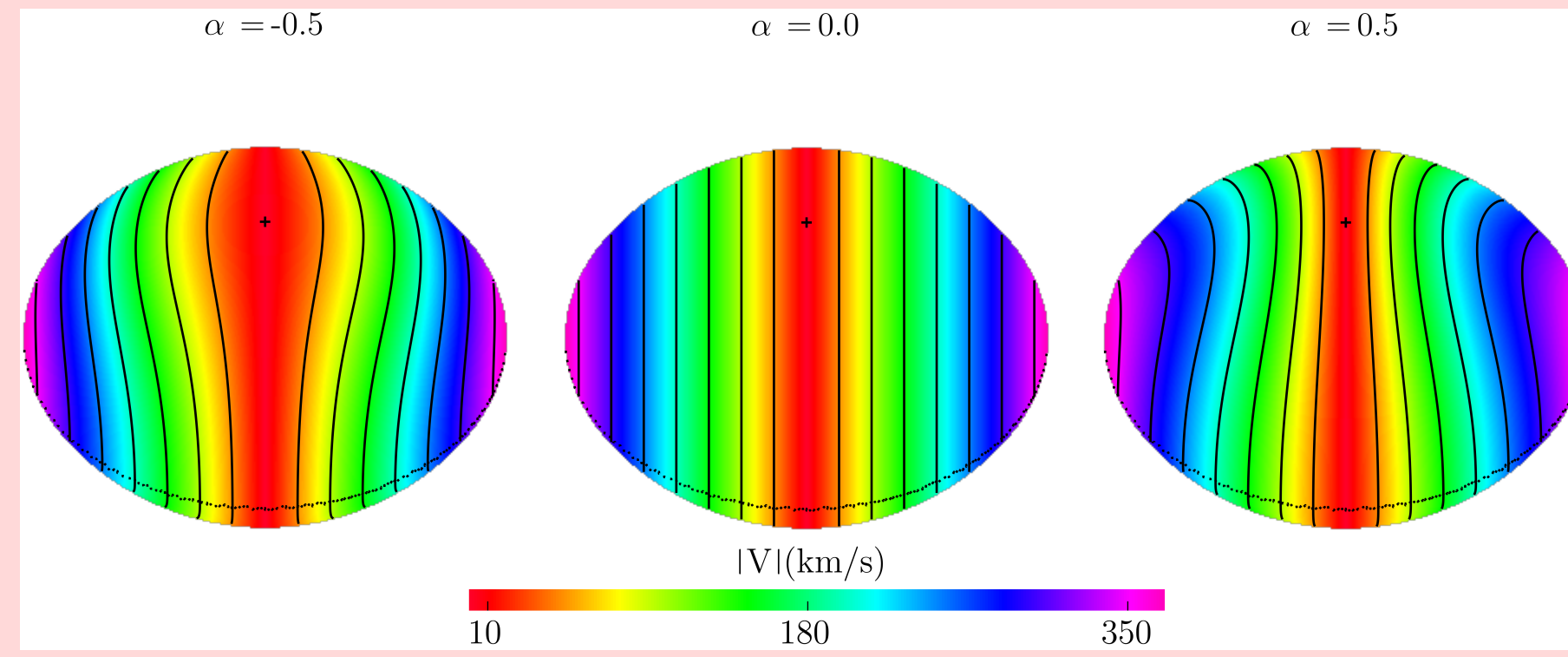


Figure 1: Deformed apparent disk computed for a star that has the following parameters: $T_{\text{eff}} = 23000$ K, $\log g = 4.1$, $\eta = 0.8$ (see Equ. 6), $i = 45^\circ$. Throughout this poster we explore 3 situations of surface differential rotation for which we draw the curves of constant radial velocity \mathcal{C} which contribute to the rotational Doppler broadening of spectral lines: $\alpha = -0.5$ (left panel), $\alpha = 0$. (rigid rotation; middle panel), and $\alpha = +0.5$ (right panel).

8. Conclusions

- One important consequence introduced by the surface differential rotation is that the gravity darkening exponent becomes a function of θ AND of α as shown in Fig. 3. Its value inferred from observations is therefore a function of the stellar inclination angle, and does not only reflect the characteristics of the stellar surface rotation.
- Differential rotation has a significant impact on line profiles and its effects vary from one line to another (Figs. 4, 5, 6, 7). We therefore expect that the phenomenon, if present, should be measurable on high SNR and high resolution spectra.
- Surface differential rotation makes classical methods for deriving $V \sin i$ unreliable, as is the case of the Fourier transform technique (Figs. 8, 9, 10, 11).

3. Gravitational Darkening Laws

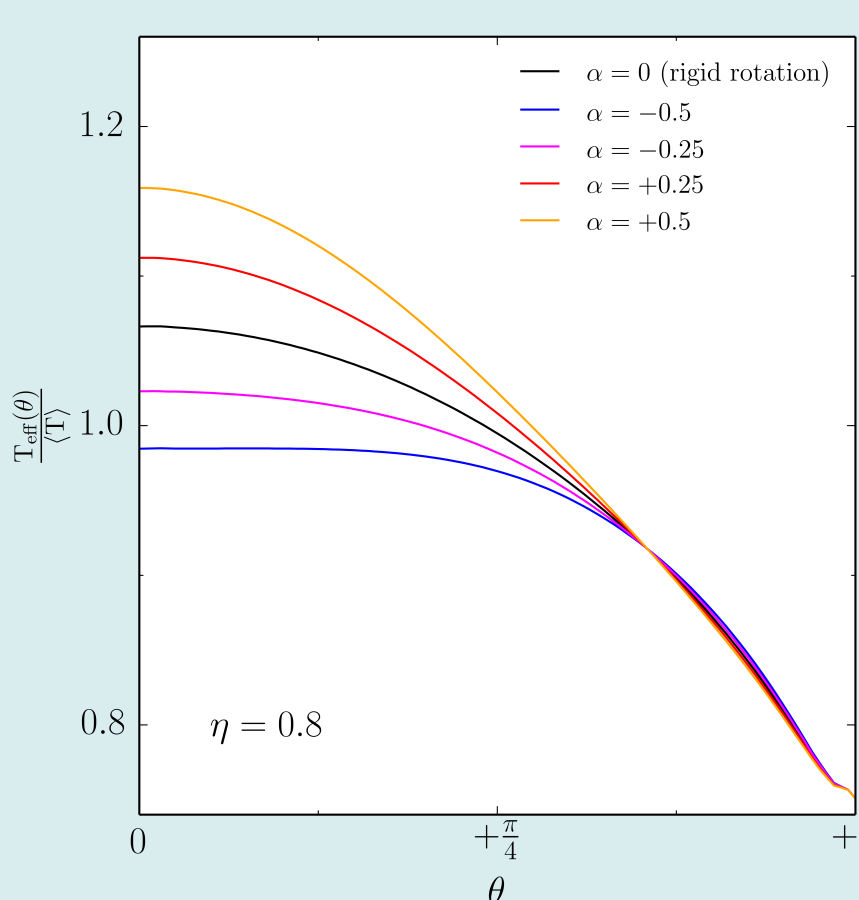


Figure 2: Normalized effective temperature as a function of the co-latitude, and computed for $\eta = 0.8$ as well as for different values of α .

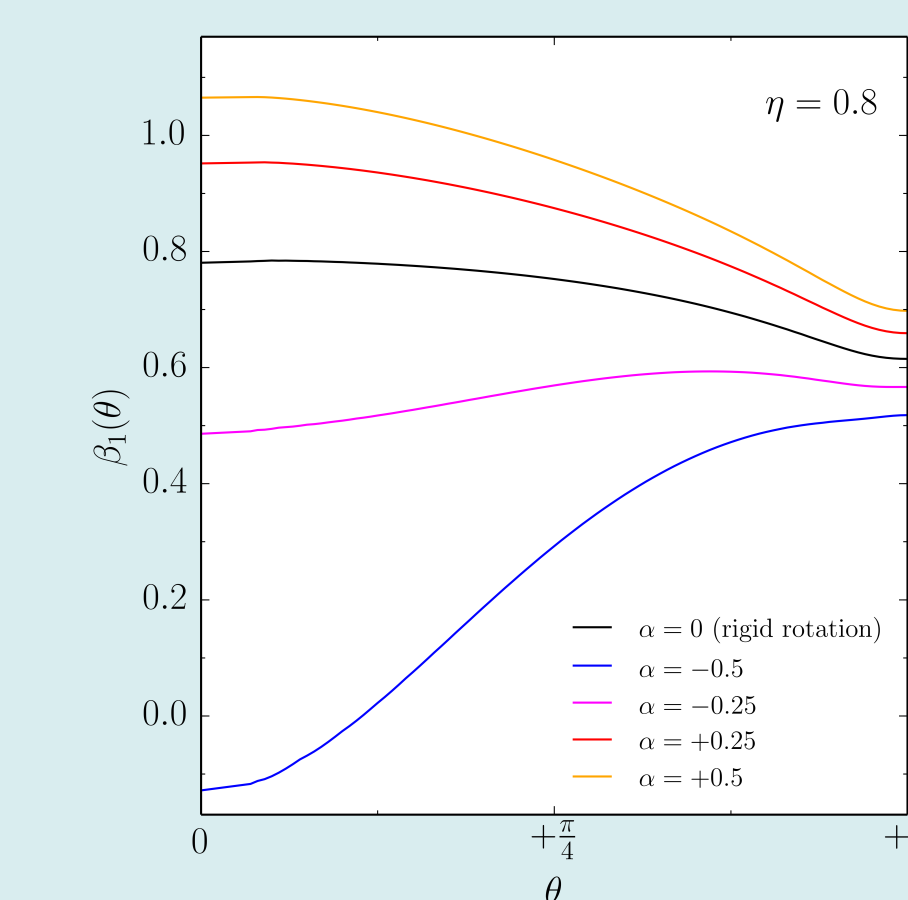


Figure 3: Gravity-darkening exponent, β_1 , against θ for $\eta = 0.8$ and for different values of α .

4. Consequences on line profiles

Another important consequence introduced by surface differential rotation is the dependence of the intensity and width of the spectral lines with the aspect angle, i , which is more complex than in the rapid rigid rotation case. This can already be deduced from the shape of the constant radial velocity \mathcal{C} curves in Fig. 1. The sensitivity of the lines to η and i depends on their sensitivity to line-formation conditions, here illustrated by the He I 4471 and Mg II 4481 lines. In Figs. 4 and 5 are compared the FWHM of these lines with those they would have in conditions of rigid rotation ($\alpha = 0$). In Figs. 6 and 7 are compared their equivalent widths (EW) with the EW they would have in conditions of rigid rotation ($\alpha = 0$).

The differential rotation introduces changes in the estimate of the $V \sin i$ parameter, which does not reflect straightforwardly the projected equatorial velocity any more. This is due to the change of the Doppler line broadening which is produced over constant radial velocity curves (Fig. 1) and not over straight lines as in rigid rotators. In this situation, the first zeroes of the line Fourier Transform (FT) (usually used to derive $V \sin i$) cannot be compared with those of the classic line broadening function derived for rigid rotators (Figs. 8 and 9). In Figs. 10 and 11 is compared the $V \sin i$ parameter derived using the FT-technique with those estimated in rigid rotators. In both cases the linear equatorial velocity is strictly the same (same η parameter).

5. Full Widths at Half Maximum

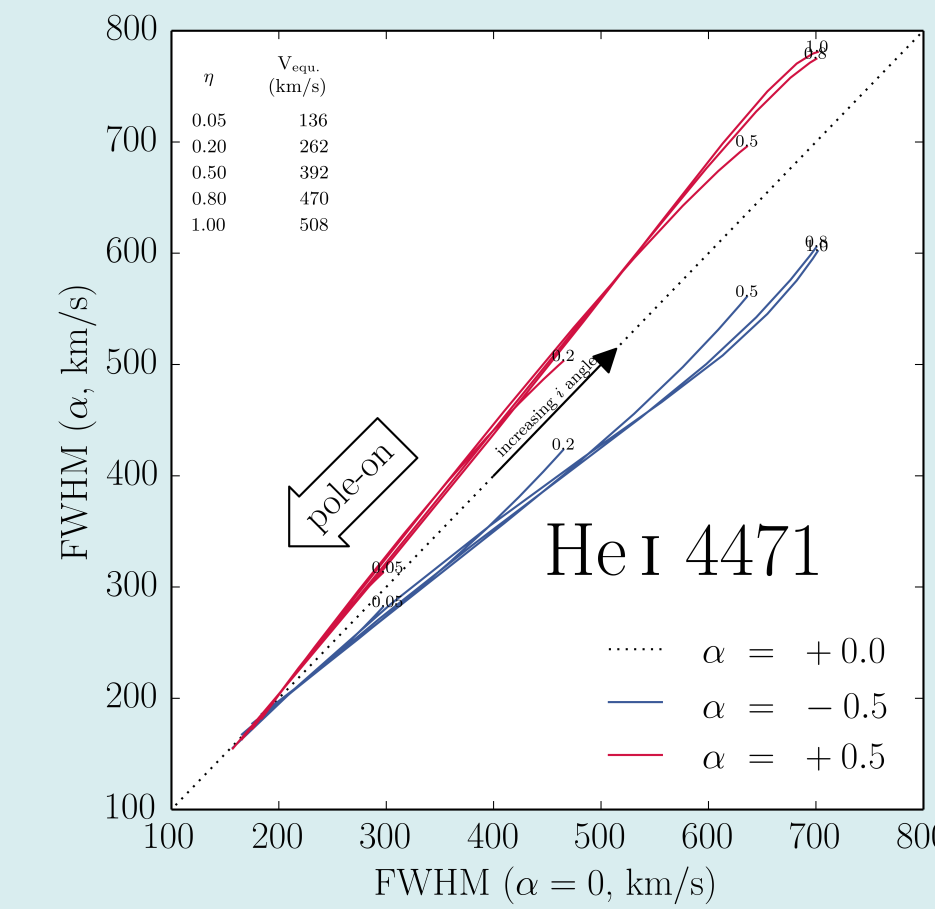


Figure 4: Full width at half maximum (FWHM) for the He I 4471 line in differential rotators against the FWHM in rigid rotators. Different values of η (values are reported on the curves, as well as given in the table inset) and of α are assumed.

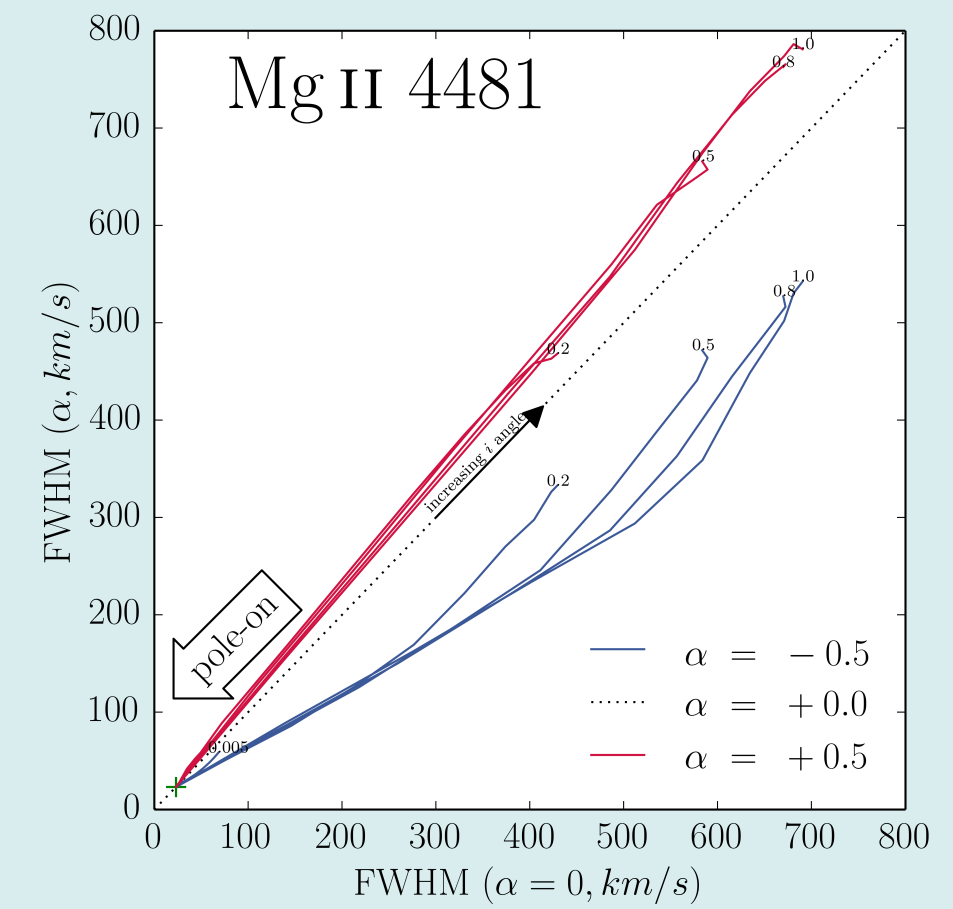


Figure 5: Full width at half maximum (FWHM) for the Mg II 4481 line in differential rotators against the FWHM in rigid rotators. Different values of η (values are reported on the curves) and of α are assumed.

6. Equivalent Width

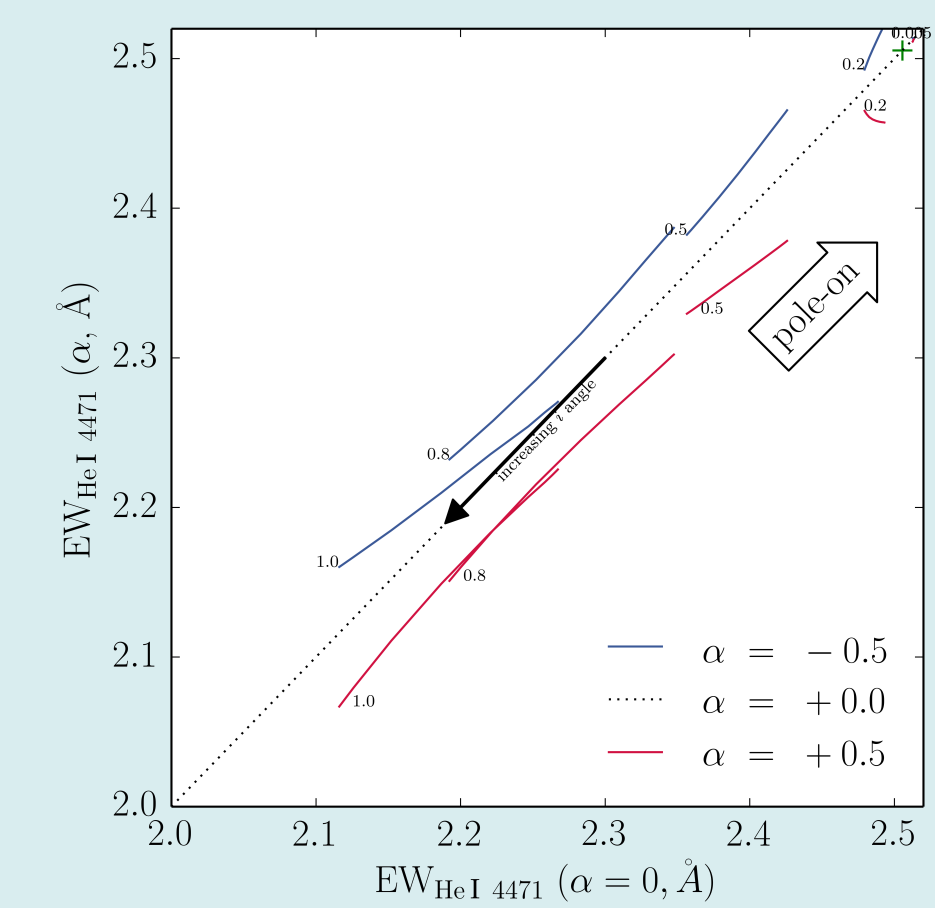


Figure 6: Equivalent width of the He I 4471 line in differential rotators against its equivalent width in rigid rotators. Different values of η (see values reported on the curves) and of α were considered.

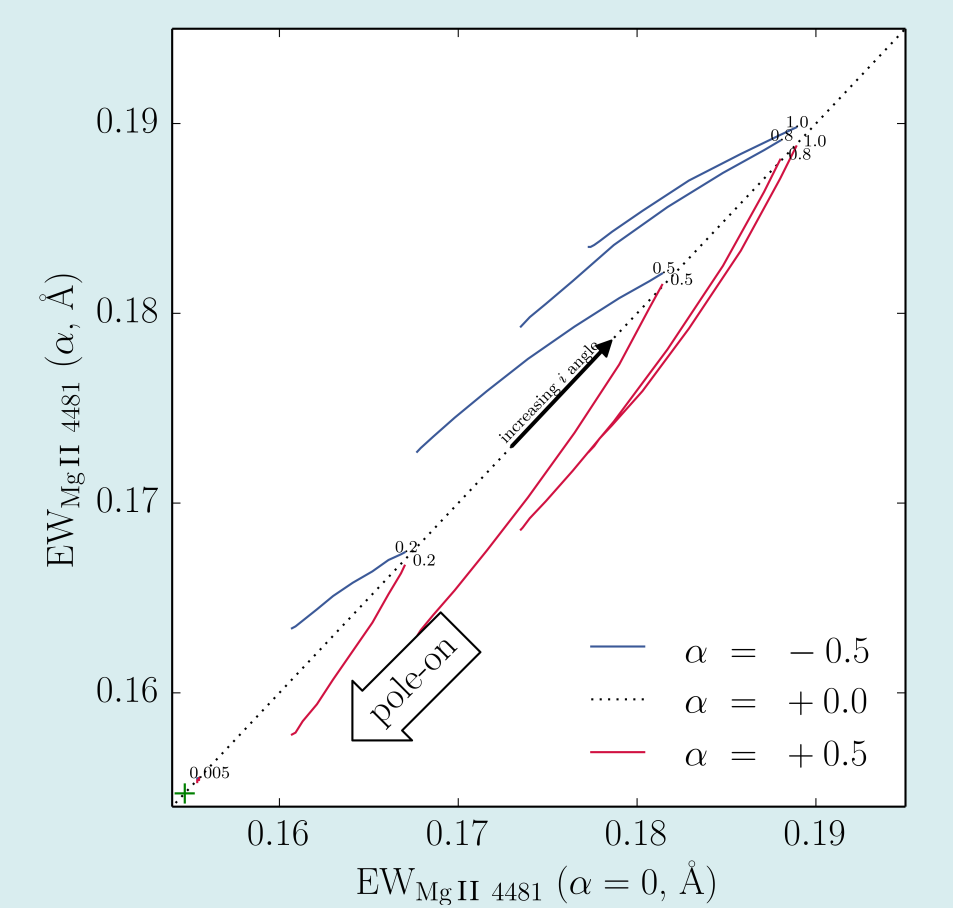


Figure 7: Equivalent width of the Mg II 4481 line in differential rotators against its equivalent width in rigid rotators. Different values of η (see values reported on the curves) and of α were considered.

7. Fourier Transform and $V \sin i$ determination

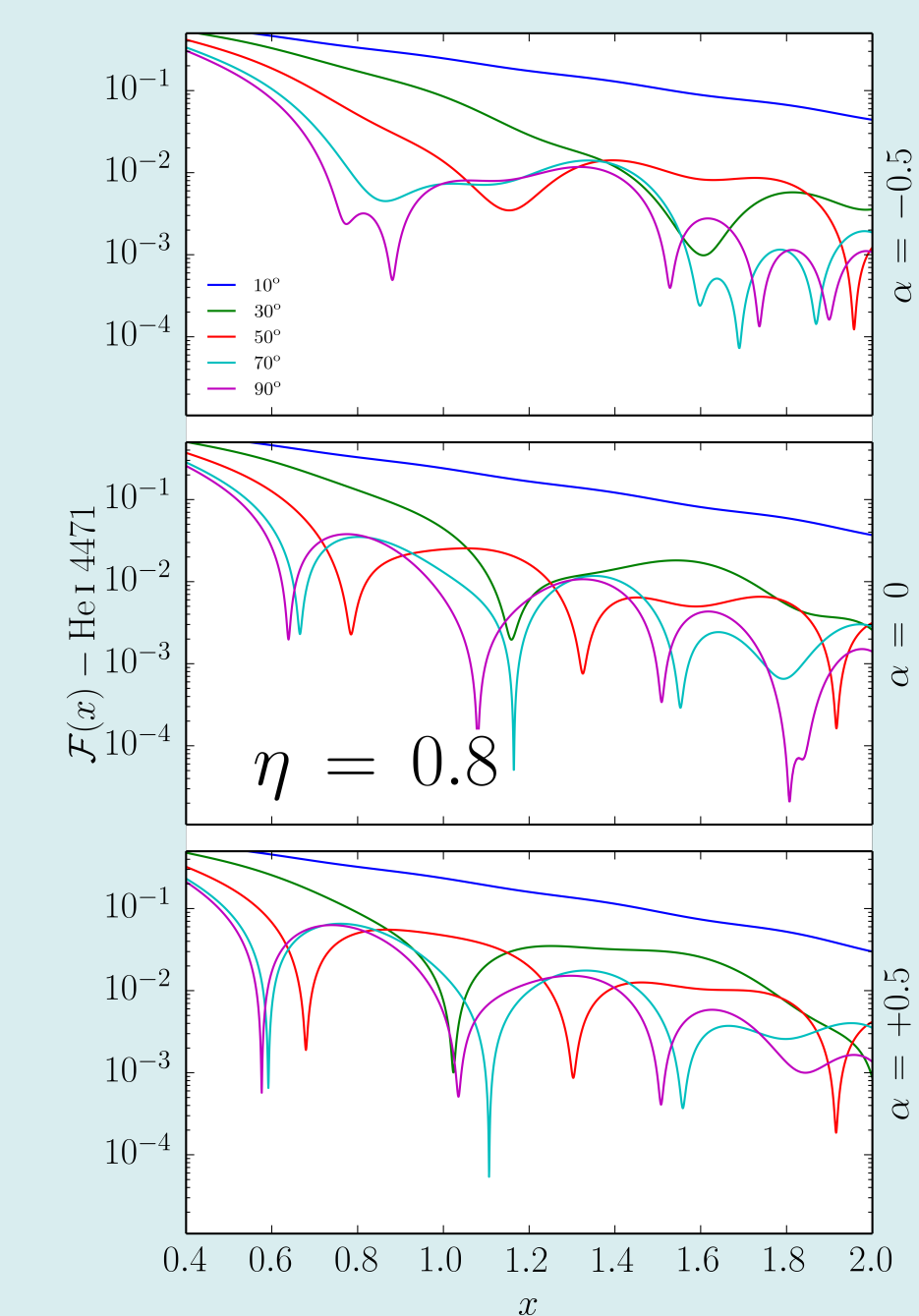


Figure 8: Fourier transform of He I 4471 in differential rotators. The computations have been made assuming $\eta = 0.8$, and for various combinations of the inclination angle and of α .

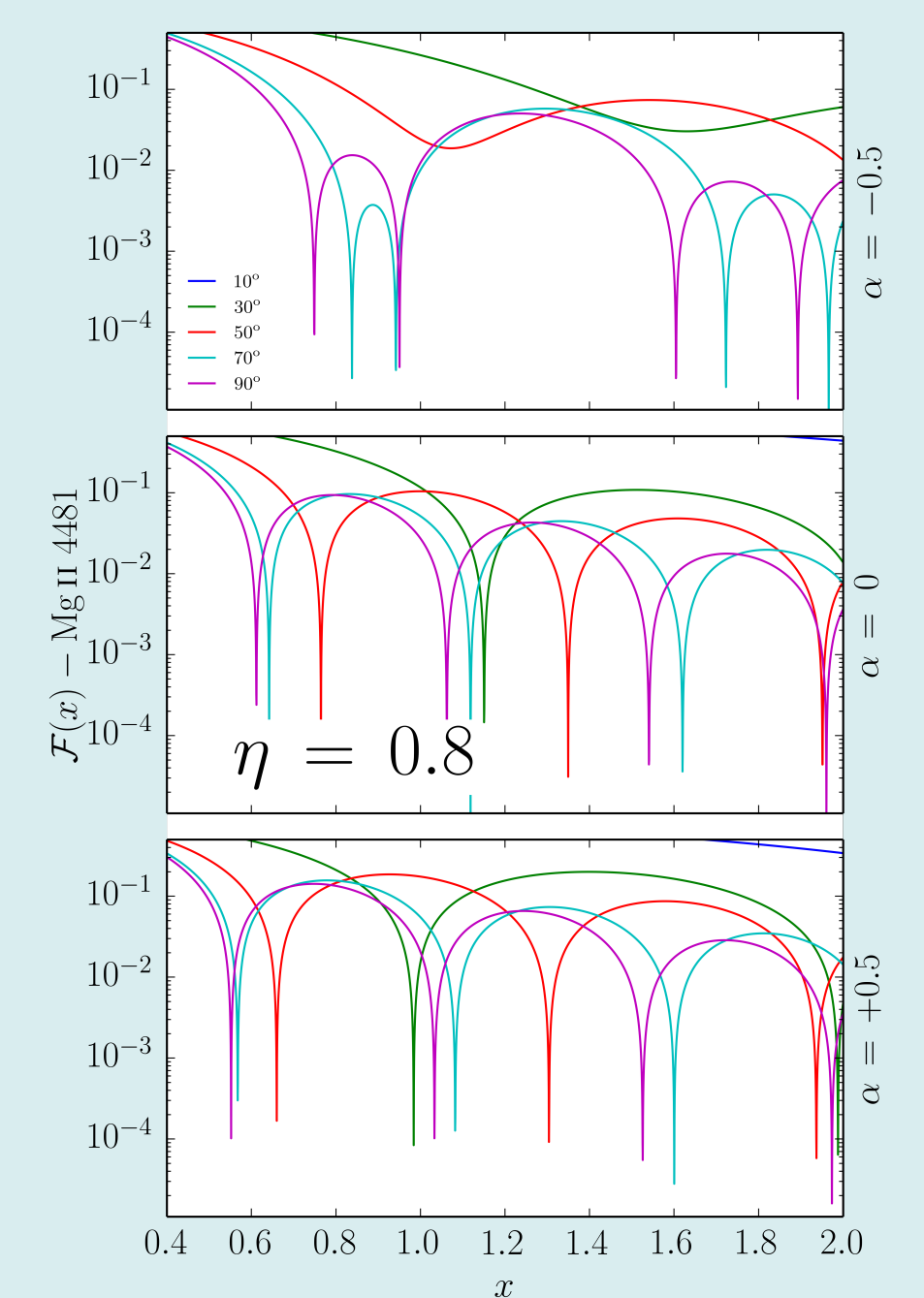


Figure 9: Fourier transform of Mg II 4481 in differential rotators. The computations have been made assuming $\eta = 0.8$, and for various combinations of the inclination angle and of α .

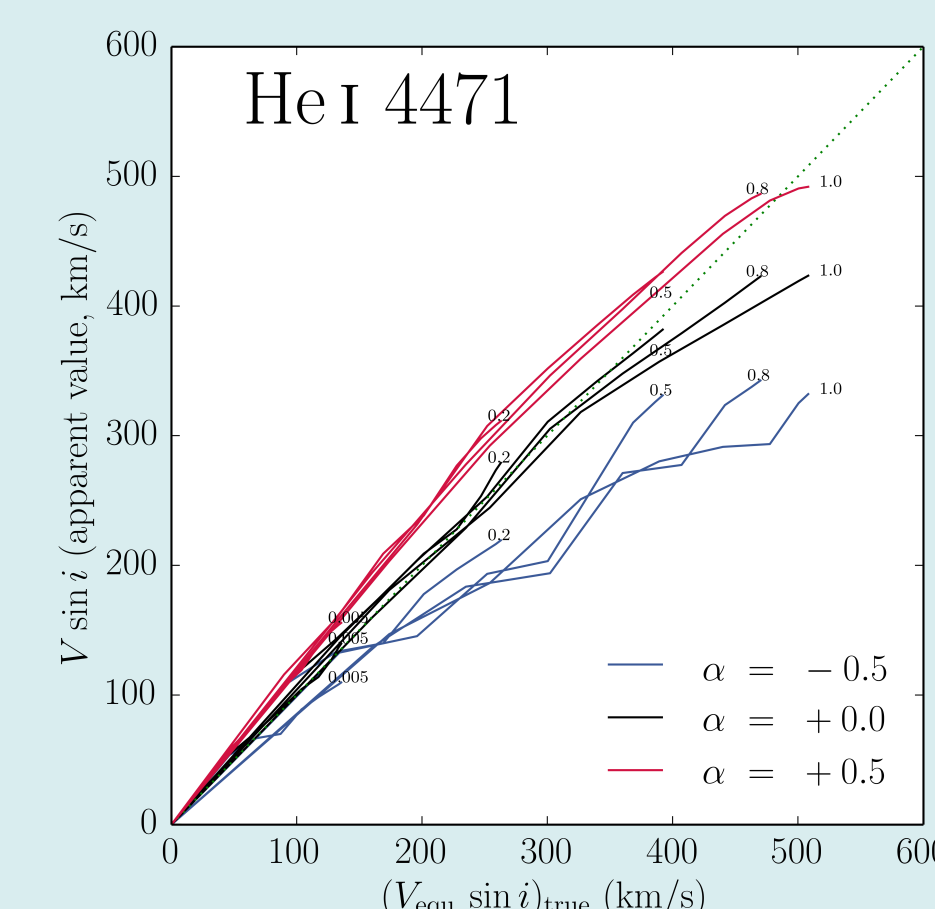


Figure 10: Measured (or apparent) $V \sin i$ derived by means of the FT technique applied on the He I 4471 line in differential rotators against the true $V \sin i$. Different values of η and of α were assumed.

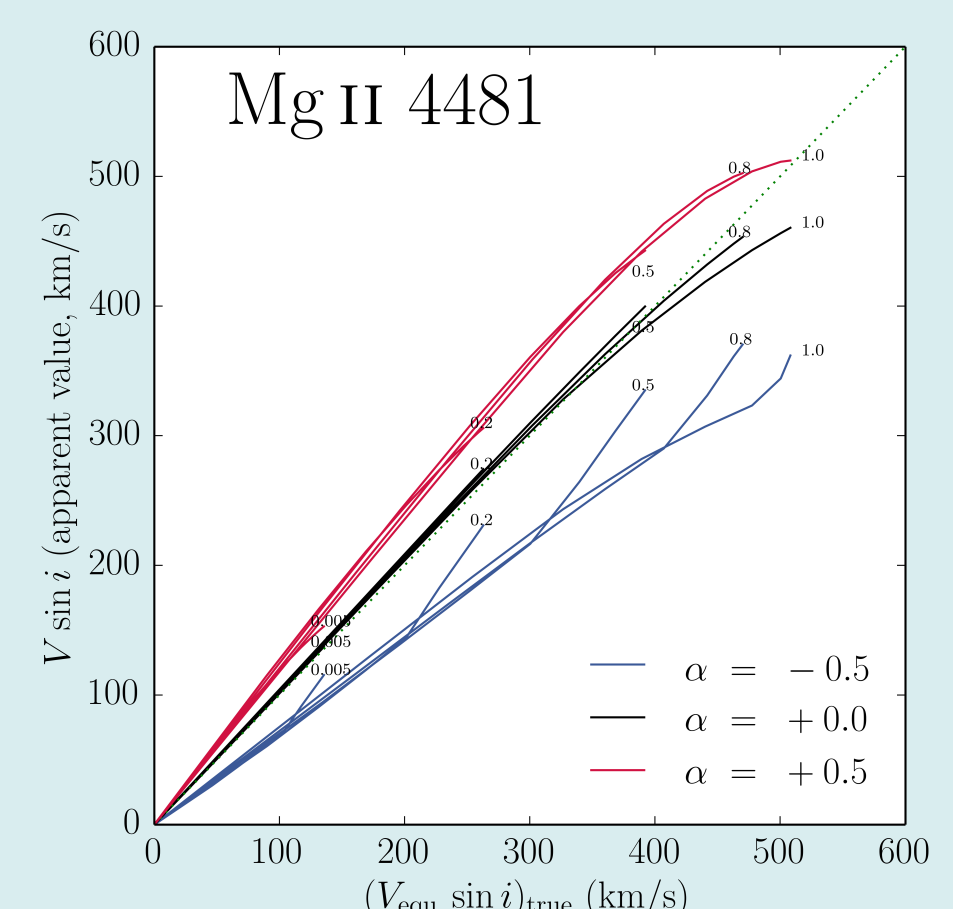


Figure 11: Measured (or apparent) $V \sin i$ derived by means of the FT technique applied on the Mg II 4481 line in differential rotators against its true $V \sin i$. Different values of η and of α were assumed.



Y. Frémat (present at this conference)
yves.fremat@observatory.be
Astronomy and Astrophysics Group
Royal Observatory of Belgium

